Journal of Orthopaedic Translation (2018) 12, 45—54

Available online at www.sciencedirect.com

ScienceDirect

journal homepage: http://ees.elsevier.com/jot

ORIGINAL ARTICLE

Comparisons of slice-encoding metal artifact correction and view-angle tilting magnetic resonance imaging and traditional digital radiography in evaluating chronic hip pain after total hip arthroplasty

Yimin Ma [a,*], Panli Zuo [b], Mathias Nittka [c], Xiaoguang Cheng [a], Hongyi Shao [d], Chen Wang [a]

[a] Department of Radiology, Jishuitan Hospital, Beijing, China
[b] Siemens Healthcare, MR Collaborations NE Asia, Beijing, China
[c] Siemens Healthcare GmbH, Erlangen, Germany
[d] Department of Orthopedics, Jishuitan Hospital, Beijing, China

Received 12 July 2017; received in revised form 15 November 2017; accepted 29 November 2017
Available online 20 December 2017

KEYWORDS
Metal artifact;
Slice-encoding metal artifact correction and view-angle tilting magnetic resonance;
Total hip arthroplasty

Abstract *Purpose:* The aims of this study were (1) to compare the areas of metal-induced artifacts and definition of periprosthetic structures between patients scanned with the slice-encoding metal artifact correction and view-angle tilting (SEMAC-VAT) turbo-spin-echo (TSE) prototype and those scanned with the standard TSE magnetic resonance (MR) sequences and (2) to further clarify the superiority of the SEMAC-VAT MR imaging technique at detecting lesions in patients after total hip arthroplasty (THA), compared with digital radiography (DR).
Materials and methods: A total of 38 consecutive patients who underwent THA were referred to MR imaging at our institution. All patients suffered from chronic hip pain postoperatively. Twenty-three patients of the 38 were examined with a 1.5-T MR scanner using a SEMAC-VAT TSE prototype and standard TSE sequence, and the remaining 15 patients were examined with the same 1.5-T MR scanner, but using the SEMAC-VAT TSE prototype only. The traditional DR imaging was also performed for all patients. Two radiologists then independently measured the area of metal-induced artifacts and evaluated the definition of both the acetabular and femoral zones based on a three-point scale. Finally, the positive findings of chronic hip pain after THA based on SEMAC-VAT TSE MR imaging and traditional DR imaging were compared and analysed.
Results: The areas of metal-induced artifacts were significantly smaller in the SEMAC-VAT TSE sequences than those in the standard TSE sequences for both the T1-weighted ($p < 0.001$) and

* Corresponding author.
E-mail address: 845547842@qq.com (Y. Ma).

https://doi.org/10.1016/j.jot.2017.11.002

T2-weighted ($p < 0.001$) turbo inversion recovery magnitude images. In addition, 28 patients showed a series of positive signs in the SEMAC-VAT images that were not observed in the traditional DR images.
Conclusion: Compared with the standard TSE MR imaging, SEMAC-VAT MR imaging significantly reduces metal-induced artifacts and might successfully detect most positive signs missed in the traditional DR images.
Translational potential of this article: The main objective of this research was to show that MR sequences from the SEMAC-VAT TSE prototype provide a significant advantage at detecting lesions in patients after THA because of the excellent soft-tissue resolution of the MR imaging. SEMAC-VAT MR can evaluate chronic hip pain after THA and determine the cause, which can help the clinician decide on whether a surgical revision is needed.

Introduction

Total hip arthroplasty (THA) is widely performed to treat orthopaedic disorders of the hip joint such as end-stage osteoarthritis, severe fractures (especially for elderly patients) and bone tumours [1]. Although THA can relieve pain, maintain stability and restore activity of the hip joint, it also brings some periprosthetic-associated complications such as periprosthetic bone resorption, periprosthetic fractures and metal implant dislocations [2,3], which can cause hip pain to reoccur. Distortion-free magnetic resonance (MR) imaging around the metal has shown the great clinical potential for assessing patients suffering from continuous hip pain after THA.

Traditionally, patients after THA often undergo routine digital radiography (DR) and an additional computed tomography (CT) scan if necessary. As a standard imaging method for evaluating the clinical outcomes of an arthroplasty procedure, DR can clearly show the shape and location of the metal implant and the periprosthetic bone status. However, it has also been reported to have relative low sensitivity and specificity [4,5]. Moreover, the clinical application of CT is limited by its heavy metal-induced artifacts, high radiation dosage and low resolution of soft tissue [6]. Therefore, the ability to optimally assess individuals after THA has become an imperative goal.

MR imaging has become an important modality for assessing musculoskeletal disorders, especially THA, due to the high sensitivity in detecting soft-tissue lesions and differentiating imaging contrasts [6,7]. However, its application on routine examinations remains unknown based on the metal-induced artifacts in patients with THA. The predominant form of metal-induced artifacts is signal loss and signal pile-up, which are caused by large resonance frequency variations of the magnetic field [8—11]. These metal-induced artifacts can generally be categorised into two types: in-plane distortions (signal displaced within the plane) and through-plane distortions (signal displaced to other planes) [12]. Recently, view-angle tilting (VAT) and slice-encoding metal artifact correction (SEMAC) MR imaging techniques have been introduced to correct both in-plane and through-plane distortions to reduce metal-induced artifacts and to extend the clinical application of MR imaging for assessing patients with metal implants [12,13]. Previous studies have validated the use of SEMAC-VAT MR imaging to assess patients with THA [14—16]. However, few studies have clarified its superiority at detecting the pathological findings in patients with chronic hip pain after THA, especially with regard to a comparison with the traditional DR imaging.

The purpose of our study was to (1) compare the areas of metal-induced artifacts and definition of periprosthetic structures between patients scanned with a SEMAC-VAT turbo-spin-echo (TSE) prototype and with the standard TSE MR sequences and to (2) further clarify the superiority of the SEMAC-VAT MR imaging technique at detecting the pathological findings of patients with chronic hip pain after THA compared with the traditional DR imaging.

Material and methods

Patients

A total of 38 consecutive patients (12 men and 26 women; mean age: 53.89 ± 13.72; range: 29—80), who underwent THA with titanium alloy (cobalt—chromium included) metal-on-metal prostheses, were referred for MR imaging between July 2014 and October 2017 at our institution. Specifically, 29 patients had undergone unilateral THA, and the remaining nine had undergone bilateral THA. Of the 38 patients, 23 were examined with a 1.5-T MR scanner using a SEMAC-VAT TSE prototype and standard TSE sequence. The remaining 15 patients were examined with the same 1.5-T MR scanner but using the SEMAC-VAT TSE prototype only. All patients suffered from chronic hip pain postoperatively for more than 3 months.

MR and DR imaging

The SEMAC-VAT TSE prototype data of all patients were obtained using a 1.5-T MR scanner (MAGNETOM Espree, Siemens Healthcare, Erlangen, Germany) and an eight-channel hip coil. The parameters of the two SEMAC-VAT prototype sequences are given below:

1. SEMAC-VAT TSE, coronal/axial T1-weighted imaging: echo-delay time (TE): 5.7 ms; repetition time (TR): 400 ms; field of view: 380 × 380 mm^2; refocusing flip angle: 150°; matrix: 320 × 320; section thickness: 4.0 mm; turbo factor: 7; readout bandwidth: 651 Hz/pixel; and encoding steps: 6.
2. SEMAC-VAT TSE, coronal/axial T2-weighted turbo inversion recovery magnitude (TIRM) imaging: TE: 51 ms; TR: 7820 ms; field of view: 380 × 380 mm^2; refocusing flip angle: 150°; matrix: 320 × 320; section thickness: 4.0 mm; turbo factor: 31; readout bandwidth: 579 Hz/pixel; and encoding steps: 6. Here, "TIRM" indicates a fat-suppressing sequence.

Standard TSE sequences were applied to the first 30 cases of postoperative hip joints (23 patients: 10 men and 13 women). These sequences were then eliminated because the resultant images exhibited heavy metal artifacts and, therefore, did not contribute to the diagnosis. However, the standard TSE sequence images constituted a baseline for comparing the artifact reductions of the two SEMAC-VAT prototype sequences. The parameters of the standard TSE sequences are listed below:

1. Standard, coronal/axial T1-weighted imaging: TE: 16 ms; TR: 484 ms; field of view: 380 × 380 mm^2; refocusing flip angle: 150°; matrix: 320 × 320; section thickness: 4.0 mm; turbo factor: 7; and readout bandwidth: 156 Hz/pixel.
2. Standard, coronal/axial T2-weighted TIRM imaging: TE: 51 ms; TR: 7450 ms; field of view: 380 × 380 mm^2; refocusing flip angle: 150°; matrix: 320 × 320; section thickness: 4.0 mm; turbo factor: 31; and readout bandwidth: 180 Hz/pixel.

In addition, all patients underwent a hip joint DR scan with a Kodak DirectView DR7500 digital X-ray machine.

Image analysis

All coronal MR images were first divided into two parts: the acetabular and femoral zones. These zones were divided by a line drawn from the superior margin of the greater trochanter to the superior margin of the lesser trochanter (Fig. 1). Then, two experienced attending musculoskeletal radiologists (both of whom have worked at our hospital for more than 10 years) independently measured the metal-induced artifact area and evaluated the definitions of both the acetabular and femoral zones based on a three-point scale (0: severe metal-induced artifacts with no delineation of prosthesis; 1: blurring in periprosthetic structures; and 2: clear delineation of prosthesis with high resolution of periprosthetic structures). Signs related to chronic hip pain after THA in the SEMAC-VAT TSE MR images and traditional DR images were further compared by the two radiologists. When their results were inconsistent, consensus was reached through consultation.

Statistical analysis

All analyses were performed with the SPSS software (IBM SPSS Inc., Chicago, IL, USA). The differences in areas of metal-induced artifacts were assessed by using the Wilcoxon signed-rank test. The differences in qualitative data were also assessed by using the Wilcoxon signed-rank test. Data were shown as the mean ± standard deviation. A p value < 0.05 was considered to be statistically significant.

Figure 1 Coronal image of a patient after THA divided into two parts (i.e., the acetabular and femoral zones) by a line drawn from the superior margin of the greater trochanter to the superior margin of the lesser trochanter.
THA = total hip arthroplasty.

Results

Table 1 summarises the descriptive statistics of the metal-induced artifacts in the coronal images. The areas of metal-induced artifacts were significantly smaller in the SEMAC-VAT TSE sequences than those in the standard TSE sequences for both the T1-weighted ($p < 0.001$) and T2-weighted TIRM images ($p < 0.001$). The mean scores were also higher in the SEMAC-VAT sequences than in the standard TSE sequences for both the T1-weighted ($p < 0.001$) and T2-weighted TIRM ($p < 0.001$) images (Table 2). Besides, the mean SEMAC-VAT imaging scores were higher in the femoral zone than in the acetabular zone, for both the T1-weighted ($p = 0.015$) and T2-weighted TIRM ($p = 0.002$) images (Table 3).

Moreover, 32 patients (45 cases of postoperative hips) showed a series of positive signs in the SEMAC-VAT images compared with those found in the traditional DR images (SEMAC-VAT/DR = n_1/n_2). These are summarised as follows: (1) periprosthetic bone resorption ($n_1/n_2 = 6/2$), (2) a synovial-like membrane surrounding the prosthesis ($n_1/n_2 = 7/2$), (3) adverse local tissue reaction (ALTR) ($n_1/n_2 = 1/0$), (4) synovitis ($n_1/n_2 = 3/0$), (5) hip muscle atrophy/oedema

Table 1 Area of metal artifacts for standard TSE and SEMAC-VAT TSE in T1-weighted and T2-weighted TIRM images.

N = 30	Acetabular zone		Femoral zone	
	Standard	SEMAC-VAT	Standard	SEMAC-VAT
Coronal T1-weighted (cm^2)	44.21 ± 19.93	23.30 ± 6.17*	26.16 ± 13.06	15.23 ± 4.29*
Coronal T2-weighted TIRM (cm^2)	46.34 ± 25.35	26.61 ± 8.02*	24.56 ± 13.19	14.41 ± 6.98*

SEMAC-VAT = slice-encoding metal artifact correction and view-angle tilting; TIRM = turbo inversion recovery magnitude; TSE = turbo-spin-echo.
Standard TSE compared with SEMAC-VAT TSE. *$p < 0.001$ for all.

($n_1/n_2 = 9/0$), (6) synovial hyperplasia ($n_1/n_2 = 11/0$) and (7) osseous stress reaction (OSR) ($n_1/n_2 = 14/0$).

Figs. 2–5 show several cases of periprosthetic bone resorption and synovial-like membrane in the SEMAC-VAT MR images. In general, periprosthetic bone resorption and synovial-like membrane lesions had similar appearances except for the difference in the width of the lesions. The following signs may indicate both lesions:

a) In the SEMAC-VAT MR images, both types of lesions appeared to be a line or band surrounding the metal implants with low-to-intermediate signals in the T1-weighted sequences and intermediate-to-high signals in the T2-weighted TIRM sequences depending on the stage of lesions. The line or band was continuous. If the width of the lesion was more than 2 mm, it was diagnosed as bone resorption; otherwise, it was a synovial-like membrane [17].
b) Marrow oedema may also exist.
c) In the traditional DR images, both bone resorption and a synovial-like membrane appeared as a continuous radiolucent line or band surrounding the metal implants. It may be easier to observe such signs at an oblique view [18].

Fig. 6 shows ALTR detected in the SEMAC-VAT MR images. A high concentration of metal ions was distributed in the joint fluid. Therefore, a diagnosis can be made if small metal debris is found within a lesion [17,19–21]. ALTR often appeared to be a soft-tissue mass, synovial hypertrophy and marrow or soft-tissue oedema in the MR images, which was hard to distinguish from infective lesions.

Fig. 7 shows one case of synovitis detected in the SEMAC-VAT MR images. It may appear as a soft-tissue mass, synovial hyperplasia or exudation. If the mass is close to the synovial tissue of the hip joint, it may be synovial derived. The shape, signal intensity and extent of synovitis varied with the different grades of lesions.

Table 3 Qualitative scores of SEMAC-VAT TSE for acetabular zone and femoral zone images.

N = 30	Acetabular zone	Femoral zone
Coronal T1-weighted	1.6 ± 0.5	1.9 ± 0.3*
Coronal T2-weighted TIRM	1.5 ± 0.5	1.9 ± 0.3**

SEMAC-VAT TSE = slice-encoding metal artifact correction and view-angle tilting turbo-spin-echo; TIRM = turbo inversion recovery magnitude.
0: severe metal-induced artifacts with no delineation of prosthesis; 1: blurring in periprosthetic structures; 2: clear delineation of prosthesis with good imaging of periprosthetic structures. *$p = 0.015$, **$p = 0.002$.

Similar to normal hip MR images, synovial hyperplasia, muscle atrophy and OSR detected in patients after THA showed high signals of the endosteum and marrow cavity and equal signals of the cortex and adjacent soft tissue in the SEMAC-VAT MR images. Periosteal reaction and thickening of the cortex could also be observed.

However, SEMAC-VAT MR failed to diagnose one case of acetabular prosthesis dislocation after THA.

Discussion

With the development of metal implant–imaging techniques, MR is now playing an important role in assessing patients with THA. More recently, distortion-free MR imaging has become one of the most accurate methods in the field of periprosthetic imaging. SEMAC-VAT MR imaging can significantly reduce the areas of metal-induced artifacts, which makes it sensitive to periprosthetic resorption, fractures and lesions derived from soft tissue. In this study, we used SEMAC-VAT MR imaging to assess patients with chronic hip pain after THA and compared the pathological findings with those found in the traditional DR images.

Table 2 Qualitative scores of standard TSE and SEMAC-VAT TSE for T1-weighted and T2-weighted TIRM images.

N = 30	Acetabular zone		Femoral zone	
	Standard	SEMAC-VAT	Standard	SEMAC-VAT
Coronal T1-weighted	0	1.6 ± 0.5*	0.2 ± 0.4*	1.9 ± 0.3*
Coronal T2-weighted TIRM	0.2 ± 0	1.5 ± 0.5*	0.4 ± 0.5*	1.9 ± 0.3*

SEMAC-VAT = slice-encoding metal artifact correction and view-angle tilting; TIRM = turbo inversion recovery magnitude; TSE = turbo-spin-echo.
0: severe metal-induced artifacts with no delineation of prosthesis; 1: blurring in periprosthetic structures; 2: clear delineation of prosthesis with good imaging of periprosthetic structures. *$p < 0.001$ for all.

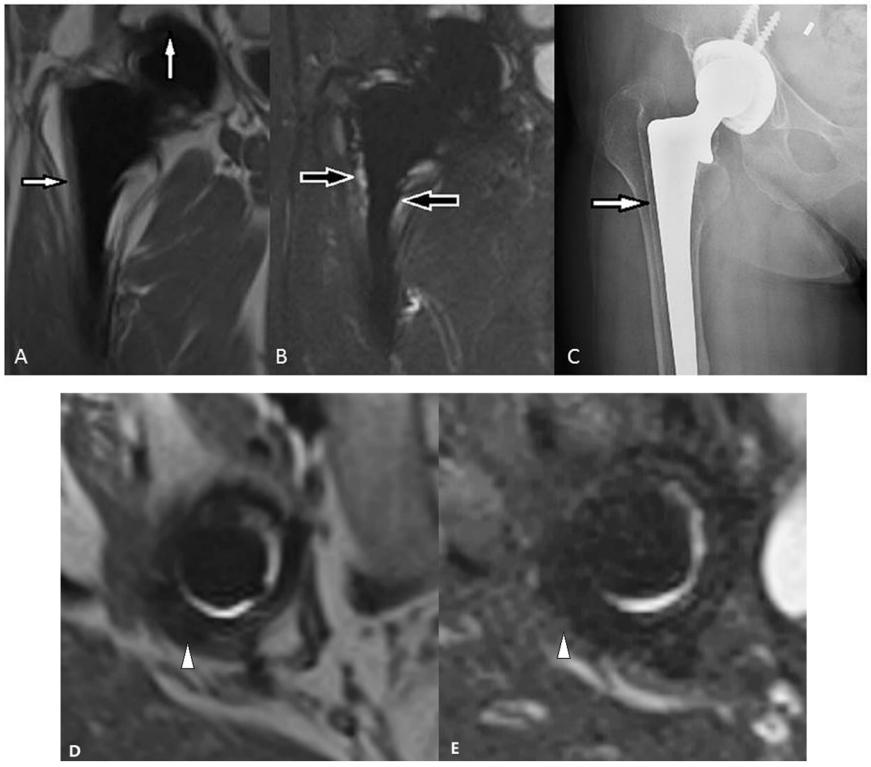

Figure 2 (A) T1-weighted SEMAC-VAT image, of a 56-year-old female who underwent THA on her right hip joint, showing an intermediate single band at the interface between the bone and implant (white arrows). (B) T2-weighted TIRM SEMAC-VAT image, of a 56-year-old female who underwent THA on her right hip joint, showing a high signal band at the interface between the bone and implant (black arrows). (C) DR image, of a 56-year-old female who underwent THA on her right hip joint, showing a radiolucent line surrounding the implant (white arrow). (D) T1-weighted SEMAC-VAT image, of a 56-year-old female who underwent THA on her right hip joint, showing an intermediate-to-low signal band surrounding the acetabular cup (white arrow head). (E) T2-weighted TIRM SEMAC-VAT image, of a 56-year-old female who underwent THA on her right hip joint, showing a low signal band surrounding the acetabular cup (white arrow head), highly suggesting bone resorption lesion. The patient was diagnosed with periprosthetic bone resorption both in acetabular and femoral zones, which was finally confirmed intraoperatively.
DR = digital radiography; SEMAC-VAT = slice-encoding metal artifact correction and view-angle tilting; THA = total hip arthroplasty; TIRM = turbo inversion recovery magnitude.

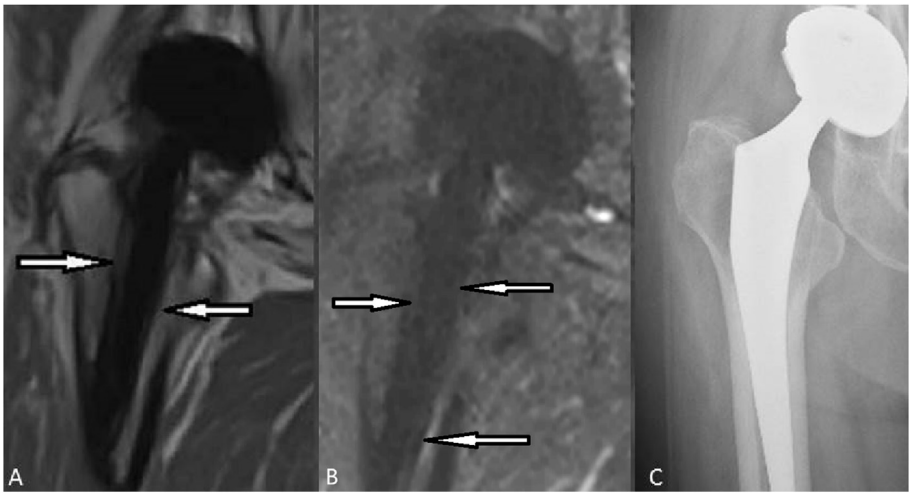

Figure 3 (A) T1-weighted SEMAC-VAT image, of a 79-year-old female who underwent THA on her right hip joint, showing an intermediate signal band at the interface between the bone and implant (white arrows) (B) T2-weighted TIRM SEMAC-VAT image, of a 79-year-old female who underwent THA on her right hip joint, showing an intermediate-to-low signal band at the interface between the bone and implant (white arrows) (C) DR image, of a 79-year-old female who underwent THA on her right hip joint, showing no significant light line surrounding the implant. The patient was diagnosed with bone resorption and a lesion on the greater trochanter side with a width of more than 2 mm. The lesion on the lesser trochanter side was diagnosed with a synovial-like membrane.
DR = digital radiography; SEMAC-VAT = slice-encoding metal artifact correction and view-angle tilting; THA = total hip arthroplasty; TIRM = turbo inversion recovery magnitude.

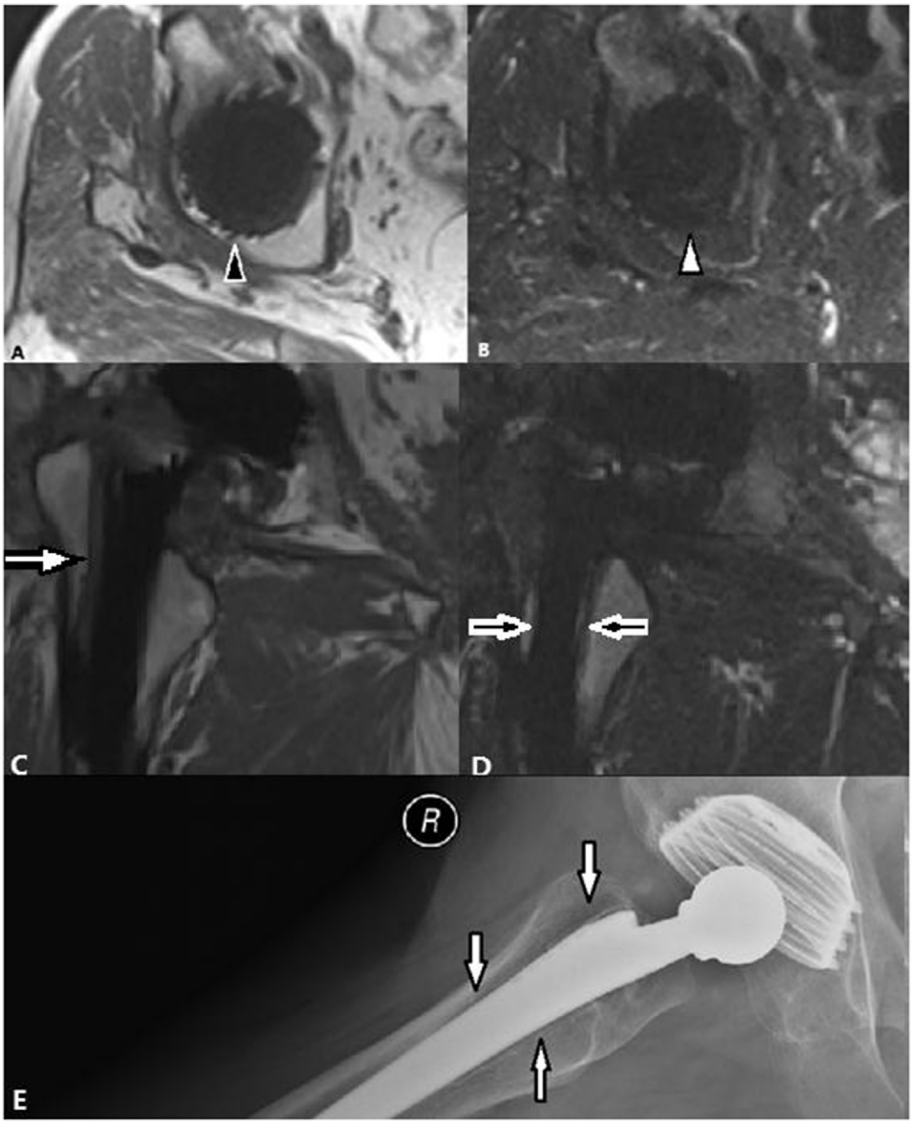

Figure 4 (A) T1-weighted SEMAC-VAT image, of a 73-year-old male who underwent THA on his right hip joint, showing a low-to-intermediate signal band at the interface between the bone and acetabular cup (black arrow head) (B) T2-weighted TIRM SEMAC-VAT image, of a 73-year-old male who underwent THA on his right hip joint, showing a low signal band surrounding the acetabular cup (white arrow head) (C) T1-weighted SEMAC-VAT image, of a 73-year-old male who underwent THA on his right hip joint, showing an intermediate signal band surrounding the metal implant (white arrow). The lesion on the lesser trochanter side was thinner than 2 mm and could not be diagnosed with bone resorption (D) T2-weighted TIRM SEMAC-VAT image, of a 73-year-old male who underwent THA on his right hip joint, showing a high signal band surrounding the metal implant (black arrows) (E) DR image, of a 73-year-old male who underwent THA on his right hip joint, showing a thin radiolucent line surrounding both the acetabular and femoral components (white arrows). Compared with the SEMAC-VAT MR image, DR underestimated the lesion on the lateral side, and we could hardly tell whether the acetabular radiolucent band in the DR image was caused by bone resorption or osteoporosis. The patient was diagnosed with bone resorption (acetabular zone and lesion on the greater trochanter side) and a synovial-like membrane (lesion on the lesser trochanter side).
DR = digital radiography; MR = magnetic resonance; SEMAC-VAT = slice-encoding metal artifact correction and view-angle tilting; THA = total hip arthroplasty; TIRM = turbo inversion recovery magnitude.

Traditional MR imaging is often interrupted by severe metal-induced artifacts resulting from large resonance frequency variations of the magnetic field. The degree of metal-induced artifacts is mainly affected by the type of implanted material, prosthesis design, strength of the static magnetic field, scanning orientation and sequence parameters [22—24]. For traditional MR sequences, a lower magnetic field may reduce metal-induced artifacts. Metal-induced artifacts are smaller for images acquired with a fast spin echo sequence than those acquired with a gradient recalled echo sequence [25—27]. For fatty suppression, images acquired with short T1 inversion recovery sequences have reduced metal-induced artifacts compared with spectral fat saturation sequences [24]. Specific sequential

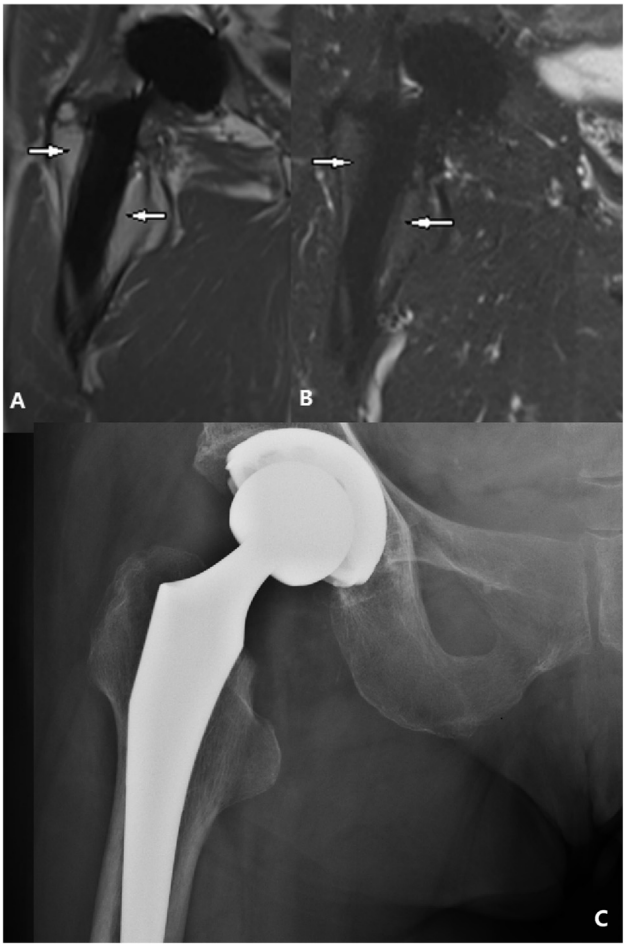

Figure 5 (A) T1-weighted SEMAC-VAT image, of a 64-year-old female who underwent THA on her right hip joint, showing a low-to-intermediate signal band at the interface between the bone and implant (white arrows). The width of the lesion was less than 2 mm (B) T2-weighted TIRM SEMAC-VAT image, of a 64-year-old female who underwent THA on her right hip joint, showing a low-to-intermediate signal band surrounding the implant (white arrows). A synovial-like membrane was diagnosed in this patient (C) DR image, of a 64-year-old female who underwent THA on her right hip joint, showing no significant light line surrounding the implant.
DR = digital radiography; SEMAC-VAT = slice-encoding metal artifact correction and view-angle tilting; THA = total hip arthroplasty; TIRM = turbo inversion recovery magnitude.

designs such as VAT and SEMAC have been reported to be more efficient in reducing both in-plane and through-plane metal-induced artifacts [12—16,22,28—30].

Compared with traditional imaging techniques such as DR, CT and standard MR, SEMAC-VAT MR has many advantages when assessing patients with THA [14—16,30]. The reduction of metal-induced artifacts and high resolution for soft tissue make it possible to detect abnormal periprosthetic signals for determining periprosthetic bone resorption, synovial-like membranes, soft-tissue mass and infections. In addition, SEMAC-VAT MR images can show lesions from different views to avoid structural overlapping. They can be used to accurately evaluate the area of abnormal tissues, which is helpful when analysing the composition of lesions.

The most common complication detected in our research was OSR. An OSR is a set of positive signs that include bone oedema, soft-tissue oedema, bone cortex thickening and periosteal reaction [31]. The main cause may be the interaction between the host bone and implants. OSR presents similar signs to those of a periprosthetic fracture. The key to differentiating between the two is that the latter shows the above signs with the presence of a fracture line. Surgical reaming and compaction techniques used to prepare the femoral marrow cavity before implantation can also cause periprosthetic signal hyperintensity, which should be differentiated from OSR [17,31]. Therefore, if a patient has recently received an implantation, care should be taken when making an OSR diagnosis.

In this study, bone resorption lesions appeared as a variety of abnormal signal intensities surrounding the implants in different patients. The signal intensity may be determined by the stage of the lesion, which may contain different histological components such as fat and fibre. In our study, we found six bone resorption cases for the hips (over 47 cases in total), with two cases confirmed by surgery or/and pathology. The signal intensity was more likely to be low for both SEMAC-VAT TSE T1 and T2 TIRM. This may suggest fibre components. Two cases of bone resorption lesions yielded intermediate T1 and high T2 TIRM signals. These signals may have been caused by other tissue components with greater water content such as granulation tissue or slight oedema.

A synovial-like membrane appears similar to bone resorption lesions in MR images [32]. Fibrous membrane formation and periprosthetic bone resorption may be qualified by the thickness of the abnormal intense layer: a $\leq$2-mm thickness represents the formation of a synovial-like membrane, and a $>$2-mm thickness (and irregularity) indicates bone resorption [17].

According to the literature, periprosthetic bone resorption is activated by a number of cytokines, including interleukin-1, interleukin-6 and prostaglandin. The synovial-like membrane is formed by the migration of synovial cells and a variety of cytokines. Those cytokines contain macrophage colony-stimulating factors, tumour necrosis factors and platelet-derived growth factors [32—34], and the synovial-like membrane itself can secrete collagenase and prostaglandin E2 to activate the osteoclasts and cause bone resorption [32—34]. Theoretically, bone resorption may lead to aseptic implant loosening or further prosthetic dislocations [17], but no previous study has found an association between a synovial-like membrane and aseptic metal implant loosening [17].

In our research, the SEMAC-VAT MR failed to diagnose one case of acetabular prosthesis dislocation, as shown in Fig. 8. In this case, the SEMAC-VAT imaging could not clearly reveal the shapes of the acetabular implants or the positional relationship between the acetabulum and femoral head components. This failure was mainly caused by the artifacts around the implants. We believe that the shape made the most significant contribution to the heavy artifacts. Acetabulum components have complex and irregular shapes, which cause heavier metal artifacts, and they are

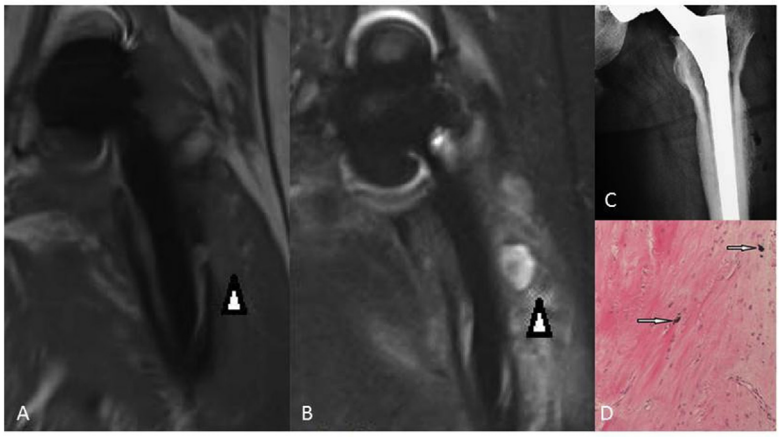

Figure 6 (A) T1-weighted SEMAC-VAT image, of a 49-year-old male who underwent THA on his left hip joint, showing nonuniform signals in the soft tissue (white arrow head). (B) T2-weighted TIRM SEMAC-VAT image, of a 49-year-old male who underwent THA on his left hip joint, showing a high signal at the soft tissue (white arrow head). (C) DR image, of a 49-year-old male who underwent THA on his left hip joint, showing suspicious lucency around the implant. However, it was not confirmed in the revision surgery, so we considered it to be a false positive. (D) Pathological findings showing fibrous hyperplasia and metallic particles (white arrows). The patient was finally diagnosed with metallosis, which is a kind of adverse local tissue reaction (ALTR).
DR = digital radiography; SEMAC-VAT = slice-encoding metal artifact correction and view-angle tilting; THA = total hip arthroplasty; TIRM = turbo inversion recovery magnitude.

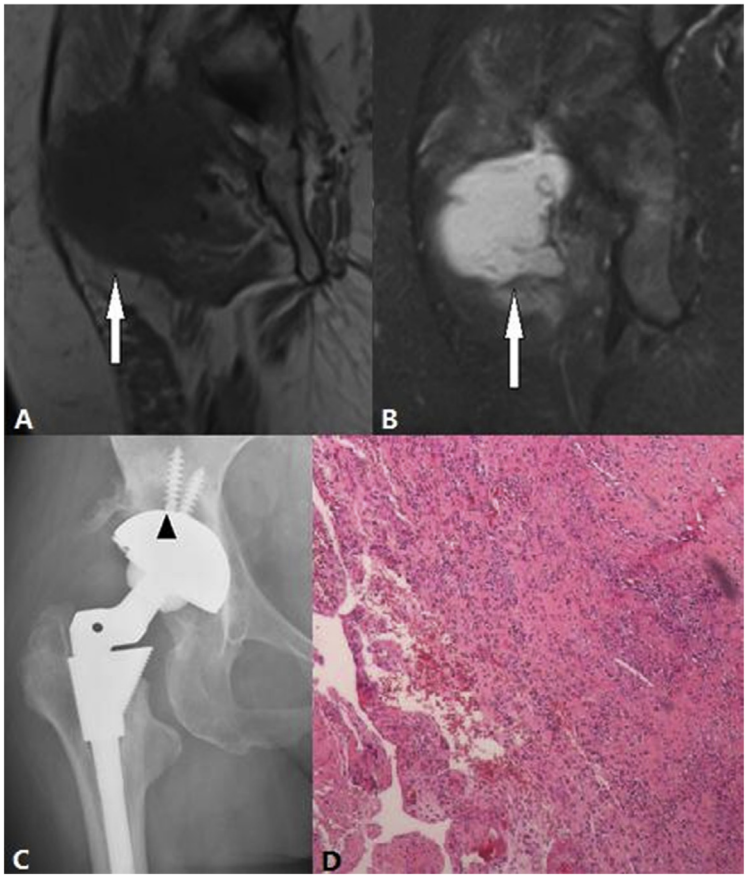

Figure 7 (A) T1-weighted SEMAC-VAT image, of a 48-year-old female who underwent bilateral THA, showing a cystic lesion with an intermediate signal that is close to the greater trochanter bursa (white arrow) (B) In the T2-weighted TIRM SEMAC-VAT image of a 48-year-old female who underwent bilateral THA, the lesion had a high signal (white arrow) (C) DR image, of a 48-year-old female who underwent bilateral THA, showing a radiolucent band surrounding the acetabular cup (black arrow head). This was not confirmed by the SEMAC-VAT MR image, which suggests osteoporosis (D) Pathological findings showing the infiltration of lymphocytes, plasma cells and neutrophils, which supports the diagnosis of chronic synovitis.
DR = digital radiography; SEMAC-VAT = slice-encoding metal artifact correction and view-angle tilting; THA = total hip arthroplasty; TIRM = turbo inversion recovery magnitude.

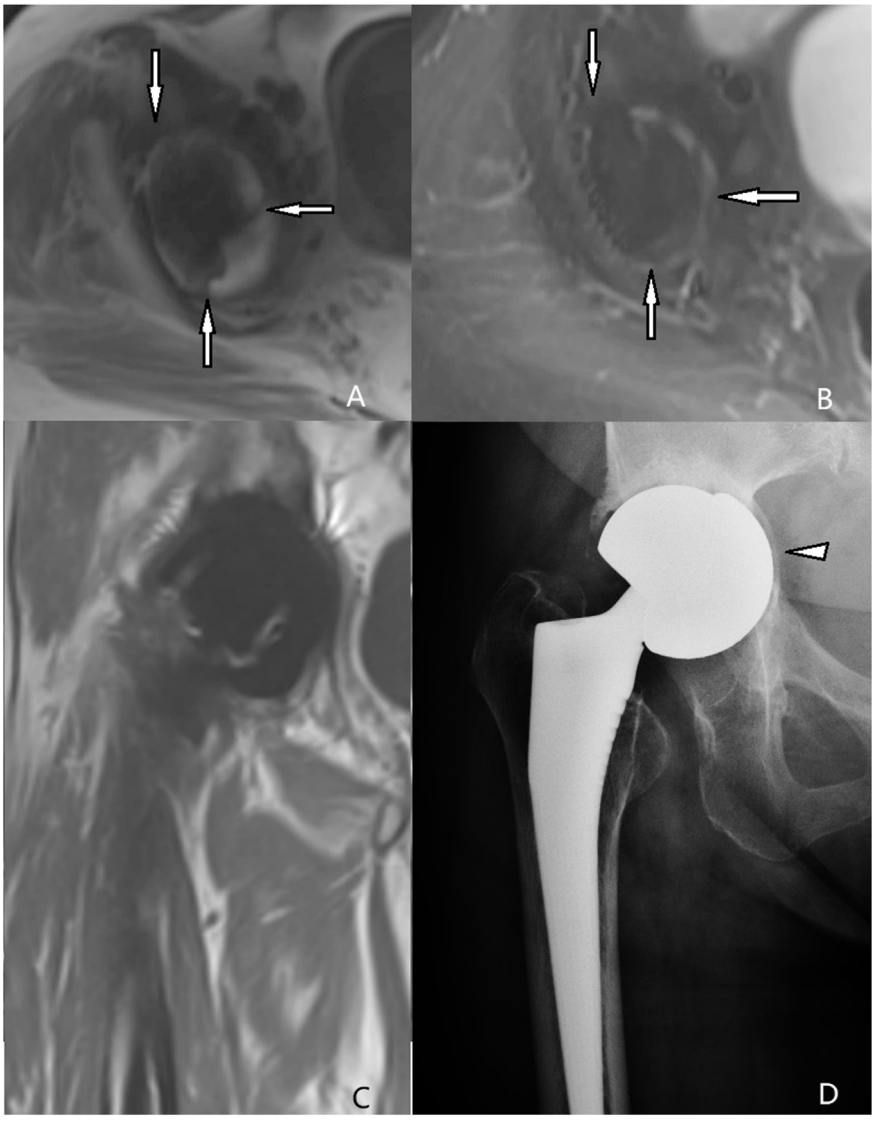

Figure 8 (A) T1-weighted SEMAC-VAT image, of a 68-year-old female who underwent bilateral THA, showing irregularly shaped low intensity around the acetabulum (white arrow), which demonstrates bone resorption for lesions more than 2 mm wide. (B) T2-weighted TIRM SEMAC-VAT image, of a 68-year-old female who underwent bilateral THA, showing irregularly shaped low intensity around the acetabulum (white arrow), which demonstrates bone resorption for lesions more than 2 mm wide (C) The coronal T1-weighted SEMAC-VAT image, of a 68-year-old female who underwent bilateral THA, showing no positive signs. (D) The DR image, of a 68-year-old female who underwent bilateral THA, showing acetabular prosthesis dislocation (white triangle).
DR = digital radiography; SEMAC-VAT = slice-encoding metal artifact correction and view-angle tilting; THA = total hip arthroplasty; TIRM = turbo inversion recovery magnitude.

more difficult to reduce [7]. Femoral head components have a regular spherical shape; therefore, we could not apply the frequency coding direction along the long axis because every axis was isometric, which may have reduced the artifacts to a certain extent [7]. These considerations may explain why the femoral zone had a significantly higher subjective score than the acetabular zone.

Our study had several limitations. First, the total scanning time of the SEMAC-VAT TSE prototype sequences was longer than that of the standard TSE sequences, which limits its clinical application for patients who are unwilling to cooperate (especially for the elderly and youth). Second, the sample size of this study was relatively small.

In conclusion, compared with the standard TSE MR imaging, SEMAC-VAT MR imaging significantly reduces metal-induced artifacts and successfully detects positive pathological findings in patients after THA which are missed by traditional DR images.

Conflicts of interest statement

One of our researchers, Mathias Nittka is an employee of Siemens Healthcare GmbH, Germany. All other authors have no conflicts of interest to declare.

Acknowledgement/funding statement

All the authors have no acknowledgements or funding to declare.

References

[1] Dorr LD, Wan Z, Longjohn DB, Dubois B, Murken R. Total hip arthroplasty with use of the Metasul metal-on-metal articulation. Four to seven-year results. J Bone Joint Surg Am 2000; 82(6):789—98.

[2] Potter HG, Nestor BJ, Sofka CM, Ho ST, Peters LE, Salvati EA. Magnetic resonance imaging after total hip arthroplasty: evaluation of periprosthetic soft tissue. J Bone Joint Surg Am 2004;86-A(9):1947—54.

[3] Toms AP, Marshall TJ, Cahir J, Darrah C, Nolan J, Donell S, et al. MRI of early symptomatic metal-on-metal total hip arthroplasty: a retrospective review of radiological findings in 20 hips. Clin Radiol 2008;63(1):49—58.

[4] Buck FM, Jost B, Hodler J. Shoulder arthroplasty. Eur Radiology 2008;18(12):2937—48.

[5] Love C, Marwin SC. Nuclear Medicine and the Infected Joint Replacement. Semin Nucl Med 2009;39(1):66—78.

[6] Robinson E, Henckel J, Sabah S, Satchithananda K, Skinner J, Hart A. Cross-sectional imaging of metal-on-metal hip arthroplasties. Can we substitute MARS MRI with CT? Acta Orthop 2014;85(6):577—84.

[7] Potter HG, Li FF, Nestor BJ. What is the Role of Magnetic Resonance Imaging in the Evaluation of Total Hip Arthroplasty? Hss Journal 2005;1(1):89—93.

[8] Ludeke KM, Roschmann P, Tischler R. Susceptibility artefacts in NMR imaging. Magn Reson Imag 1985;3(4):329—43.

[9] Viano AM, Gronemeyer SA, Haliloglu M, Hoffer FA. Improved MR imaging for patients with metallic implants. Magn Reson Imag 2000;18(3):287—95.

[10] Camacho CR, Plewes DB, Henkelman RM. Nonsusceptibility artifacts due to metallic objects in MR imaging. J Magn Reson Imag 1995;5(1):75—88.

[11] Hargreaves BA, Worters PW, Pauly KB, Pauly JM, Koch KM, Gold GE. Metal-induced artifacts in MRI. AJR Am J Roentgenol 2011;197(3):547—55.

[12] Cho ZH, Kim DJ, Kim YK. Total inhomogeneity correction including chemical shifts and susceptibility by view angle tilting. Med Phys 1988;15(1):7—11.

[13] Lu W, Pauly KB, Gold GE, Pauly JM, Hargreaves BA. SEMAC: Slice Encoding for Metal Artifact Correction in MRI. Magn Reson Med 2009;62(1):66—76.

[14] Sutter R, Ulbrich EJ, Jellus V, Nittka M, Pfirrmann CW. Reduction of metal artifacts in patients with total hip arthroplasty with slice-encoding metal artifact correction and view-angle tilting MR imaging. Radiology 2012;265(1):204—14.

[15] Muller GM, Lundin B, Von ST, Muller MF, Ekberg O, Mansson S. Evaluation of metal artifacts in clinical MR images of patients with total hip arthroplasty using different metal artifact-reducing sequences. Skeletal Radiol 2015;44(3):353—9.

[16] Müller GM, Mansson S, Muller MF, Von ST, Nittka M, Ekberg O. MR imaging with metal artifact-reducing sequences and gadolinium contrast agent in a case-control study of periprosthetic abnormalities in patients with metal-on-metal hip prostheses. Skeletal Radiol 2014;43(8):1101—12.

[17] Fritz J, Lurie B, Miller TT, Potter HG. MR imaging of hip arthroplasty implants. Radiographics A Rev Publ Radiol Soc North Am Inc 2014;34(4):E106.

[18] Hodgkinson JP, Shelley P, Wroblewski BM. The correlation between the roentgenographic appearance and operative findings at the bone-cement junction of the socket in Charnley low friction arthroplasties. Clin Orthop Relat Res 1988; 228(228):105—9.

[19] Amstutz HC, Duff MJL, Campbell PA. Complications after metal-on-metal hip resurfacing arthroplasty. Orthop Clin N Am 2011;42(2):207—30.

[20] Campbell P, Ebramzadeh E, Nelson S, Takamura K, De SK, Amstutz HC. Histological features of pseudotumor-like tissues from metal-on-metal hips. Clin Orthop Relat Res 2010;468(9): 2321—7.

[21] Willert HG, Buchhorn GH, Fayyazi A, Flury R, Windler M, Koster G, et al. Metal-on-metal bearings and hypersensitivity in patients with artificial hip joints. A clinical and histomorphological study. J Bone Joint Surg Am Vol 2005;87(1): 28—36.

[22] Butts K, Pauly JM, Gold GE. Reduction of blurring in view angle tilting MRI. Magn Reson Med 2005;53(2):418—24.

[23] Graf H, Steidle G, Martirosian P, Lauer UA, Schick F. Metal artifacts caused by gradient switching. Magn Reson Med 2005; 54(1):231—4.

[24] Vandevenne JE, Vanhoenacker FM, Parizel PM, Butts PK, Lang RK. Reduction of metal artefacts in musculoskeletal MR imaging. JBR-BTR 2007;90(5):345—9.

[25] Petersilge CA, Lewin JS, Duerk JL, Yoo JU, Ghaneyem AJ. Optimizing imaging parameters for MR evaluation of the spine with titanium pedicle screws. AJR Am J Roentgenol 1996; 166(5):1213—8.

[26] Eustace S, Goldberg R, Williamson D, Melhem ER, Oladipo O, Yucel EK, et al. MR imaging of soft tissues adjacent to orthopaedic hardware: techniques to minimize susceptibility artefact. Clin Radiol 1997;52(8):589—94.

[27] Tartaglino LM, Flanders AE, Vinitski S, Friedman DP. Metallic artifacts on MR images of the postoperative spine: reduction with fast spin-echo techniques. Radiology 1994;190(2):565—9.

[28] Lu W, Pauly KB, Gold GE, Pauly JM, Hargreaves BA. Slice encoding for metal artifact correction with noise reduction. Magn Reson Med 2011;65(5):1352—7.

[29] Lee YH, Lim D, Kim E, Kim S, Song HT, Suh JS. Usefulness of slice encoding for metal artifact correction (SEMAC) for reducing metallic artifacts in 3-T MRI. Magn Reson Imaging 2013;31(5):703—6.

[30] Mansson S, Muller GM, Wellman F, Nittka M, Lundin B. Phantom based qualitative and quantitative evaluation of artifacts in MR images of metallic hip prostheses. Phys Med 2015;31(2): 173—8.

[31] Walde TA, Weiland DE, Leung SB, Kitamura N, Sychterz CJ, Engh Jr CA, et al. Comparison of CT, MRI, and radiographs in assessing pelvic osteolysis: a cadaveric study. Clin Orthop Relat Res 2005 2005;437:138—44.

[32] Goldring SR, Schiller AL, Roelke M, Rourke CM, O'Neil DA, Harris WH. The synovial-like membrane at the bone-cement interface in loose total hip replacements and its proposed role in bone lysis. J Bone Joint Surg Am Vol 1983;65(5): 575—84.

[33] Bosetti M, Masse A, Navone R, Cannas M. Biochemical and histological evaluation of human synovial-like membrane around failed total hip replacement prostheses during in vitro mechanical loading. Mater Sci Mater Med 2001;12(8):693—8.

[34] Thornhill TS, Ozuna RM, Shortkroff S, Keller K, Sledge CB, Spector M. Biochemical and histological evaluation of the synovial-like tissue around failed (loose) total joint replacement prostheses in human subjects and a canine model. Biomaterials 1990;11(1):69—72.